Karlsruher Institut für Technologie

Strength measurement on silica soaked in hot water

Open Access am KIT

by Susanne Wagner[1], Dominic Creek[1], Michael J. Hoffmann[1], Gabriele Rizzi[1], Sheldon M. Wiederhorn[2], Theo Fett[1]

KIT SCIENTIFIC WORKING PAPERS 23

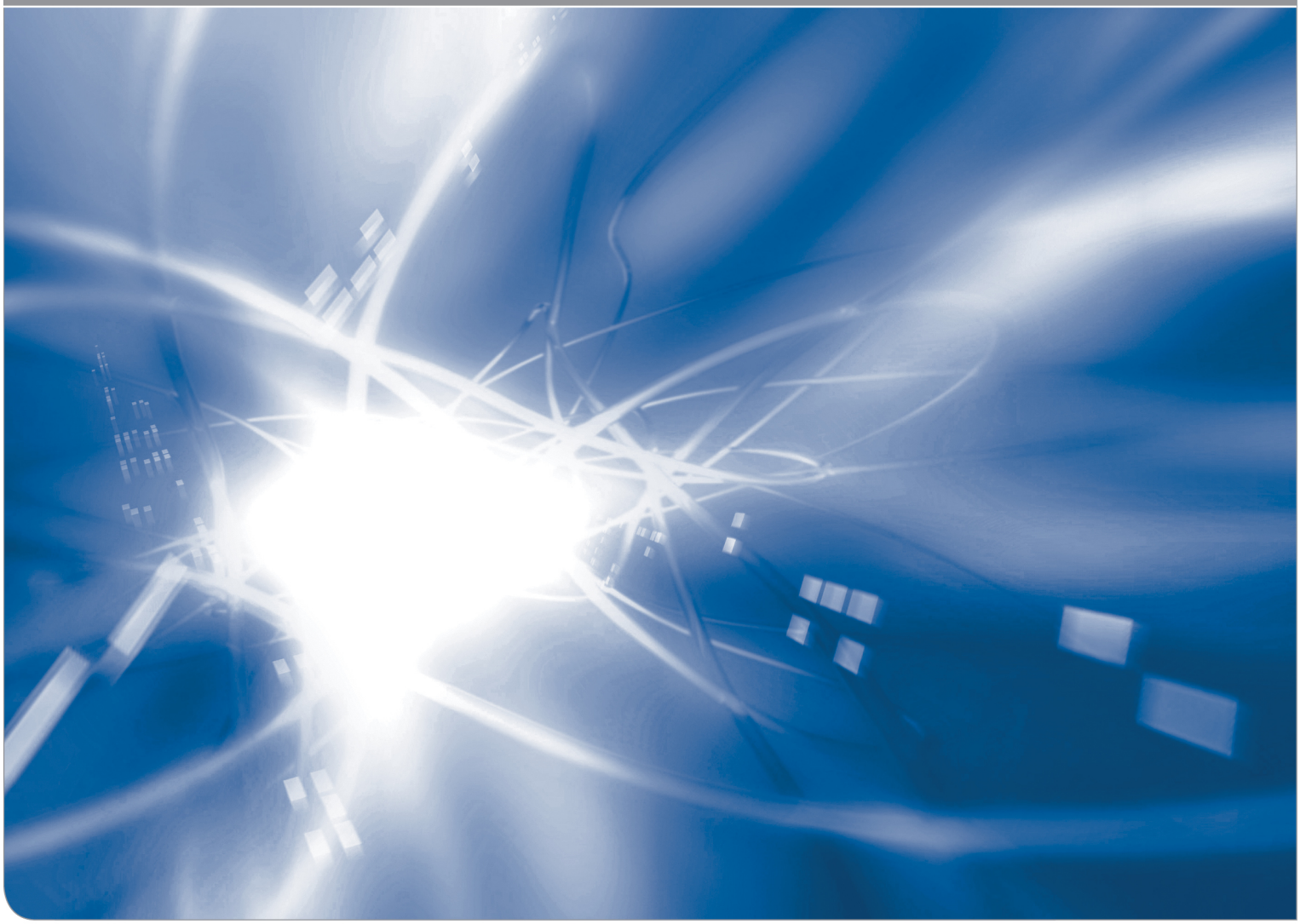

KIT – Universität des Landes Baden-Württemberg und nationales Forschungszentrum in der Helmholtz-Gemeinschaft

[1]Institut für Angewandte Materialien, Karlsruher Institut für Technologie (KIT)

[2]National Institute of Standards and Technology, Gaithersburg, MD

Impressum

Karlsruher Institut für Technologie (KIT)
www.kit.edu

2014

ISSN: 2194-1629

Abstract

The effect of water soaking on the strength of silica glass is studied. When silica glass is immersed in warm water and held there for an extended period of time, the strength increases over that of freshly damaged glass. The increase in strength is a consequence of water diffusion into exposed surfaces of the test specimen, which results in swelling of the glass and shielding of cracks present in the surface of the glass.

In our first paper on this subject (Report 19 of this series), we considered swelling effects on the inert strength. In the present report, the strength under subcritical crack growth conditions is studied.

For tests carried out in humid environment at various loading rates, so-called dynamic strength tests, we could show theoretically that the swelling effect caused by the reaction of water with silica must result in apparently increased crack-growth exponents. This prediction is in good agreement with results from literature.

In our experiments we could show via an evaluation of the crack extension that even in silicone oil environment local subcritical crack growth occurs.

Contents

1. Introduction

In earlier publications [1, 2, 3, 4], we explored the idea that water can toughen silica glass by diffusing into the glass structure from the crack tip. This process sets up a negative stress intensity factor that shields the crack tip and enhances the strength of the specimen. Because diffusion rates increase with temperature, crack tip shielding should also intensify as the temperature is increased, as should the specimen strength. The effects of water diffusion on inert strength at a low soaking temperature, 90 °C, were minimal; a measured increase in strength was only about 10 %. In this paper, we address the same phenomenon, but at a higher temperature, 250 ºC.

Strength measurements at 250°C are in principle known from literature. Li and Tomozawa [5] soaked silica bars for up to 4 days and measured the strengths using dynamic bending tests in the presence of water, which enhances subcritical crack growth. Exposure to water at 250 °C enhanced the strength even in the presence of water.

In [6] we considered the effect of water toughening on the strength of silica that was tested in an inert environment. The temperature of exposure of the silica was as high as 250 °C. Strength increases depended on the time and temperature of exposure. Experimental results were found to be in agreement with theoretical estimates of strength enhancement due to water penetration of the silica surfaces bounding the crack tip. In this report, we consider the effect of water toughening on strength in the presence of subcritical crack growth.

1.1 Water Diffusion into Silica

Water diffusion into the surface of silica glass has been studied experimentally by a number of investigators, and shown to depend on temperature according to the following equation:

$$D_W = A_o \exp[-Q_W/R\Theta] \tag{1}$$

where Q_w is the activation energy for diffusion, $\Theta = (T+273°)$ is the absolute temperature, and R is the universal gas constant. From reference [7] for silica, Q_w = 72.3 kJ/mol, $\log_{10} A_0 = 8.12$ (A_0 is in m^2/s) for the *effective* diffusivity in the temperature range 0 °C to 200 °C).

The diffusion distance b, is an appropriate measure for the thickness of the diffusion zone. At b the water concentration is roughly half of that at the surface:

$$b = \sqrt{D_w t} \tag{2}$$

The parameter, t, is the time after the first contact with water.

The water in the diffusion zone reacts with the silica network according to the chemical reaction:

$$\equiv\text{Si-O-Si}\equiv + H_2O \leftrightarrow \equiv\text{SiOH}+\text{HOSi}\equiv. \tag{3}$$

The water, H_2O, is fully mobile, and the hydroxyl groups, ≡SiOH, are immobile at 250°C, fixed at the point of reaction with the silica network. If the concentration of the hydroxyl groups is $S = [\equiv\text{SiOH}]$, and the concentration of the molecular water is $C = [H_2O]$, then the sum of the two species of "water", C_w, gives the total water solubility:

$$C_w = C + \tfrac{1}{2} S \tag{4}$$

Water diffusion into the surface of silica glass in the temperature range of $23°\text{C} \le T \le 200°\text{C}$ was studied experimentally by Zouine *et al.* [7]. From their paper and a derivation by Fett *et al.* [4], the hydrogen concentration and the water concentration at the surface can be calculated as

$$C_w \cong \tfrac{1}{2} 1.15 \times 10^{20} cm^{-3} \exp[0.009T] \tag{5}$$

The ratio S/C as a function of temperature defines the equilibrium constant, k:

$$k \equiv \frac{S}{C} = A \exp\left(\frac{-Q_1}{R\Theta}\right), \tag{6}$$

with the parameters, $A = 32.3$, and $Q_1 = 10.75$ kJ/mol [10].

One would normally expect a binary reaction for the reverse direction of Eq. 3, but at low temperatures, < 300 °C, the ≡SiOH groups that form as a consequence of the reaction are fixed to the silica network, and the reverse reaction can occur only by reaction of the original adjacent ≡SiOH. Because of this restriction, the reverse reaction behaves as a first order reaction with regard to ≡SiOH. At high temperatures, > 500 °C the ≡SiOH are free to move to a limited extent and the reaction behaves as a second order reaction. Doremus discussed the order of this reaction in some detail [8]; Oehler and Tomozawa gave the experimental observations that are the basis for these conclusions [9].

1.2 Swelling of Silica

From measurements of bending moments by Wiederhorn *et al.* [10] it can be concluded that water in silica glass results in a swelling strain ε_v

$$\varepsilon_v = \frac{S/2}{C + S/2} 1.84 C_w \cong 0.00147 \frac{S/2}{C + S/2} \exp[0.009T], \tag{7}$$

as derived in [4].

A volume element near the surface that undergoes swelling cannot freely expand. If the diffusion zone is small compared to the component dimensions, expansion is completely prevented in the surface plain and can only take place normal to the surface. This results in a compressive equi-biaxial swelling stress at the surface,

$$\sigma_0 = -\frac{\varepsilon_v E}{3(1-\nu)}\ , \tag{8}$$

where E is Young's modulus and ν is Poisson's ratio. The swelling stress, σ_0, is not a material specific quantity. Due to the proportionality between the swelling stress and the hydroxyl content, $\sigma_0 \propto S$, swelling is time dependent as can be seen for soaking at 250°C from results by Oehler and Tomozawa [9], and those of Wiederhorn *et al.* [10]

2 Dynamic strength assuming edge-crack like defects

2.1 Surface defects modeled by edge cracks

The most transparent description of crack-growth problems can be given by using a solution for one-dimensional edge cracks. Under an applied remote stress, σ_{app}, the related applied stress intensity factor is

$$K_{appl} = 1.122\sqrt{\pi a}\,\sigma_{appl}\ . \tag{9}$$

The shielding stress intensity factor for an edge crack of depth a is given by [4]

$$K_{sh} \cong 1.122\sqrt{\pi a}\,\sigma_0 \tanh^{3/2}\left([0.385\sqrt{\frac{b}{a}} + 0.832\frac{b}{a}]^{2/3}\right), \tag{10}$$

with the thickness of the swelling zone b given by Eq. 2. The crack-tip stress intensity factor results by superposition of the applied and shielding stress intensity factors:

$$K_{tip} = K_{appl} + K_{sh},\ \textit{where}\ K_{sh} < 0\ . \tag{11}$$

2.2 Crack fully embedded in the swelling zone

If the crack is *fully embedded* in the swelling stress zone, *i.e.*, if $a \ll b$, it can be shown from Eqs. 9 – 11that:

$$K_{tip} = 1.122(\sigma_{appl} + \sigma_0)\sqrt{\pi a}\ . \tag{12}$$

Let us describe the subcritical crack growth rate, v, by a power law relation,

$$v = \frac{da}{dt} = AK_{tip}^n = A(K_{appl} + K_{sh})^n\ . \tag{13}$$

In the absence of swelling, $\sigma_0 = 0$ and $K_{sh} = 0$, the following well-known equation holds [11]:

$$\sigma_{f,0}^{n+1} = B\sigma_{c,0}^{n-2}\dot{\sigma}(n+1), \quad B = \frac{2K_{Ic}^{2-n}}{1.122^2\,\pi\, A(n-2)}. \tag{14}$$

The subscripts $_0$ in $\sigma_{f,0}$ and $\sigma_{c,0}$ stand for absence of swelling.

In the presence of swelling, we obtain the following equations:

$$(\sigma_f + \sigma_0)^{n+1} = B\sigma_c^{n-2}\dot{\sigma}(n+1) \tag{15}$$

$$\sigma_f = \underbrace{(B\sigma_c^{n-2}(n+1))^{1/(n+1)}\dot{\sigma}^{1/(n+1)}}_{\sigma_{f,0}} - \sigma_0 \tag{16}$$

$$\Rightarrow \sigma_f = \sigma_{f,0} - \sigma_0 \tag{16a}$$

Since the *inert strength* in soaked specimens is

$$\sigma_c = \frac{K_{Ic} - K_{sh}}{1.122\sqrt{\pi a_0}} \tag{17}$$

whereas in un-soaked specimens the *inert strength* is

$$\sigma_{c,0} = \frac{K_{Ic}}{1.122\sqrt{\pi a_0}} \tag{18}$$

where a_0 = the initial crack depth. It follows that the swelling stress is defined by

$$\sigma_0 = \sigma_{c,0} - \sigma_c\,. \tag{19}$$

Two conclusions can be drawn from Eq. 16a and Eq. 19:

Strength increase

Since the inert strength after soaking exceeds that without soaking, an increase of strength in humid environment results equal to the increase of the inert strength

$$\sigma_f - \sigma_{f,0} = \sigma_c - \sigma_{c,0} \tag{16b}$$

Apparent power-law exponent n'

Whereas for the un-soaked material the exponent in the power-law relation, n, can simply be obtained from the slope of the $\sigma_f = f(\dot{\sigma})$ plot, this is no longer possible for the water-soaked material as can be easily shown. Let us consider Eq. 16 in the following form

$$\sigma_f = \lambda \dot{\sigma}^{1/(n+1)} + \sigma_c - \sigma_{c,0} \tag{16c}$$

with the abbreviation

$$\lambda = (B\sigma_c^{n-2}(n+1))^{1/(n+1)} \tag{20}$$

A straight-line evaluation of Eq. 16c results in an apparent crack exponent n' defined by

$$\sigma_f = |\sigma_0| + \lambda \dot{\sigma}^{1/(n+1)} \Rightarrow \sigma_f \propto \dot{\sigma}^{1/(n'+1)} \tag{21}$$

i.e.

$$\frac{1}{n'+1} = \frac{d(\log \sigma_f)}{d(\log \dot{\sigma})} = \frac{d[\log(\lambda \dot{\sigma}^{1/(n+1)} + |\sigma_0|)]}{d(\log \dot{\sigma})} \tag{22}$$

By using logarithmic derivations, $d(\log x) = (1/x)\, dx$, we obtain the following equation:

$$n' = n + (n+1)\frac{\sigma_c - \sigma_{c,0}}{\sigma_{f,0}} = n + (n+1)\frac{\sigma_f - \sigma_{f,0}}{\sigma_{f,0}} \ . \tag{23}$$

Since $|\sigma_0| > 0$, it follows that $n' > n$. Thus, the apparently increased n'-value is an artifact of the logarithmic representation of a shift of a straight line by a constant value $|\sigma_0|$.

2.3 Crack partially embedded in the swelling zone

The treatment for crack sizes competing with the swelling zone size is rather complicated and nontransparent, since it requires numerical computations. One reason for this complication is the fact that the swelling stresses are now no longer constant but decrease from a maximum value at the surface continuously with increasing distance from the surface, roughly given as

$$\sigma_{sw} \cong \sigma_0 \,\mathrm{erfc}\left[\frac{z}{2b}\right] \tag{24}$$

Due to the lower swelling stresses, $|\sigma_{sw}| \le |\sigma_0|$, the inert strength σ_c and the strength σ_f are reduced from their potential full value. As a consequence of the large n-value for silica ($n > 20$), eq.(13) makes clear that the largest stress increments $d\sigma_{appl}$ per crack length increment da occurs at $a \approx a_0$, where spontaneous failure starts in the inert strength tests.

It is therefore suggested to apply Eq. 23 furthermore as a tenable approximation

$$n' \approx n + (n+1)\frac{\sigma_f - \sigma_{f,0}}{\sigma_{f,0}} \tag{23a}$$

As an example of application Eq. 23a, we discuss the results of Li and Tomozawa [5], who investigated the effect of temperature on the dynamic fatigue behavior of silica glass for soaking at 250°C under saturated vapor pressure. All their strength measurements were

performed at room temperature, in air at a relative humidity of 15 % to 30 %. The material tested was a grade of industrial silica, TO8, Heraeus-Amersil Inc. The strength data after different soaking times are in Fig. 1a.

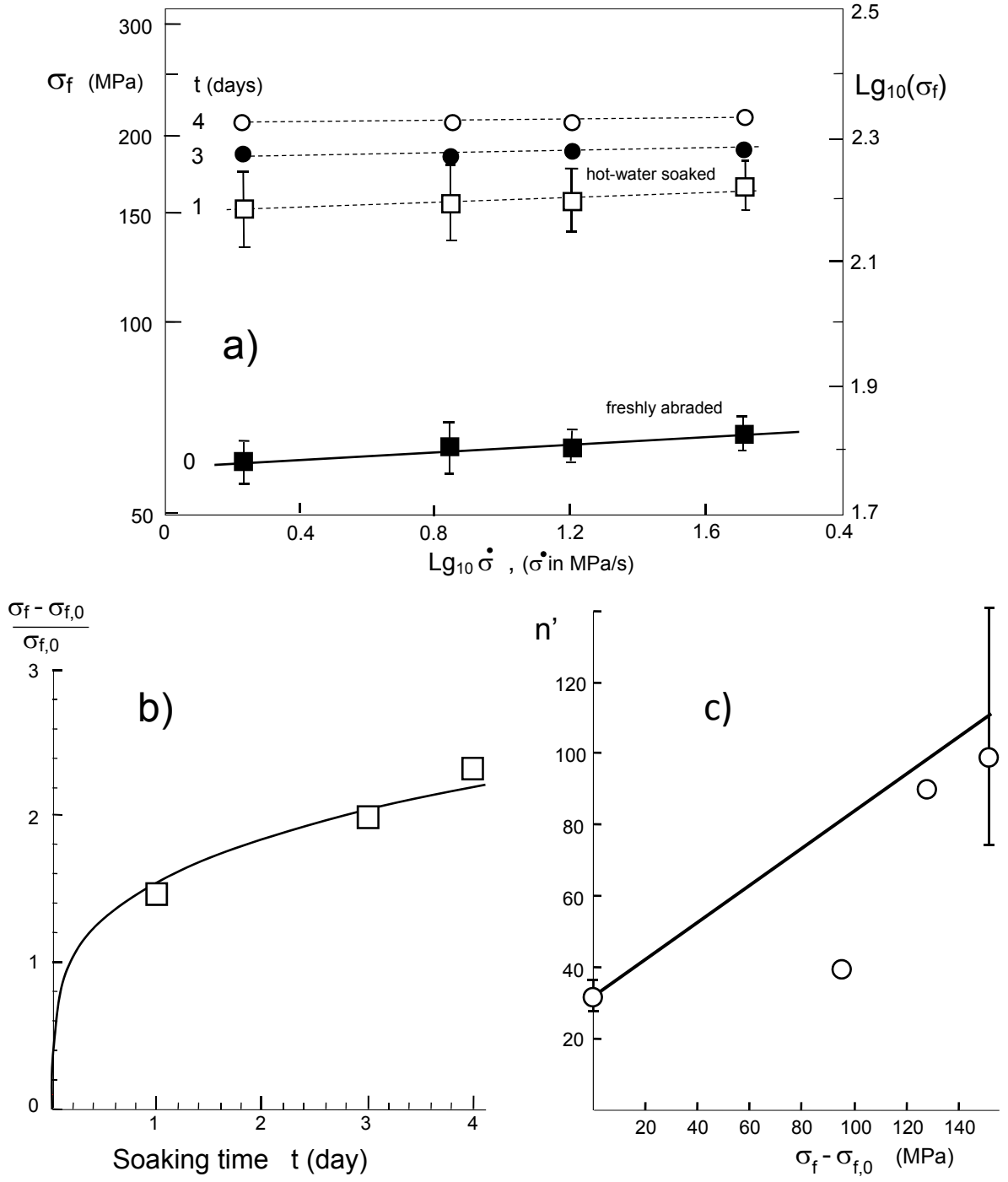

Fig. 1 a) Dynamic bending strength tests by Li and Tomozawa [5] (for clarity only a few scatter bars are introduced), b) normalized increase of dynamic strength versus heat-treatment time at 250°C; Squares: results from [5], curve: tentatively introduced guide line to the squares representing a dependency $\propto\sqrt{b} \propto t^{1/4}$, c) n'-values reported in [5] (circles), straight line: eq.(23a).

The dynamic strength measurements are plotted in Fig. 1b in form of normalized strength increments as functions of exposure time, t (squares in Fig. 1b). The curve is tentatively introduced as a guideline to the squares representing a soaking-time dependency of $t^{1/4}$ since $K_{sh} \propto \sqrt{b} \propto t^{1/4}$.

A further interesting result found by Li and Tomozawa [5] was the observation that the crack growth exponent of the v-K_{Ic} curve, n', increased with exposure time. The circles in Fig. 1c show the reported exponents as a function of the strength increase for a stress rate of $d\sigma_{appl}/dt$ = 10 MPa/s. The perpendicular bars represent the standard deviations for soaking times of t = 0 and 4 days as reported in [5]. The straight line shows the predictions by Eq. 20a.

For comparison, we have to take into account the large data scatter in Fig. 1c, and, consequently, a large uncertainty of the experimental n'-values. Nevertheless, this diagram clearly shows that with increasing strength, the crack growth exponent also increases as expected from Eq. 20a.

3. Strength measurements on silica EN80NB

3.1 Material and specimens

We studied strength behaviour of the silica glass EN08NB (GVB, Herzogenrath) containing 99.98% SiO_2. Bending bars 3×4×45 mm^3 were cut out of a plate 350×350×4 mm^3 and surface machined by peripheral grinding with a grinding wheel, D91-C75 (Effgen Gmb, Herrstein, Germany).

To eliminate residual surface stresses introduced by grinding, specimens we annealed our specimens in a vacuum for 1h at 1150 °C. The series for strength measurements in an inert environment was immediately stored in fresh silicon oil as an inert medium after cooling to room temperature, following the procedure of Sglavo and Green [12]. In our tests, we used the original silicon oil (Wacker AK 100, Wacker-Chemie AG, München), without an additional drying procedure. Each test series was carried out with fresh oil.

3.2 Strength measurements in silicon oil

3.2.1 Freshly abraded specimens

Four-point bending strength tests with the normal rectangular bending bars were made in silicone oil, as recommended by Sglavo and Green [12]. These investigators dried silica glass rods at 120°C for 2h before being completely immersed and fractured in a silicone oil bath. This procedure was considered in [12] to be an inert environment, preventing the access of water to the crack tip.

In all the tests the loading rate was 50N/s (42 MPa/s) resulting in test durations of 2-3 seconds. The average strength of 15 tests, series 1, Fig. 2, resulted in σ_c=103.5 MPa (SD 9.2 MPa). Figure 3 shows a typical example of a fracture surface.

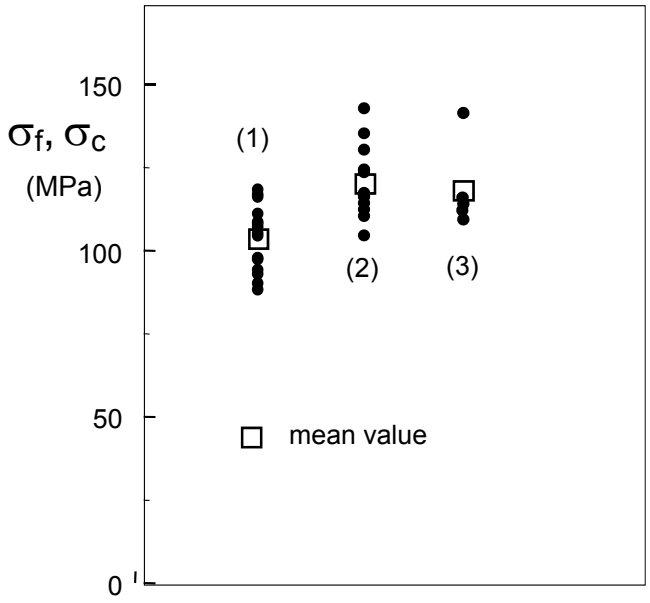

Fig. 2 Bending strength of annealed and water-soaked silica measured in silicon oil under different test conditions, (the abscissa is without physical meaning).

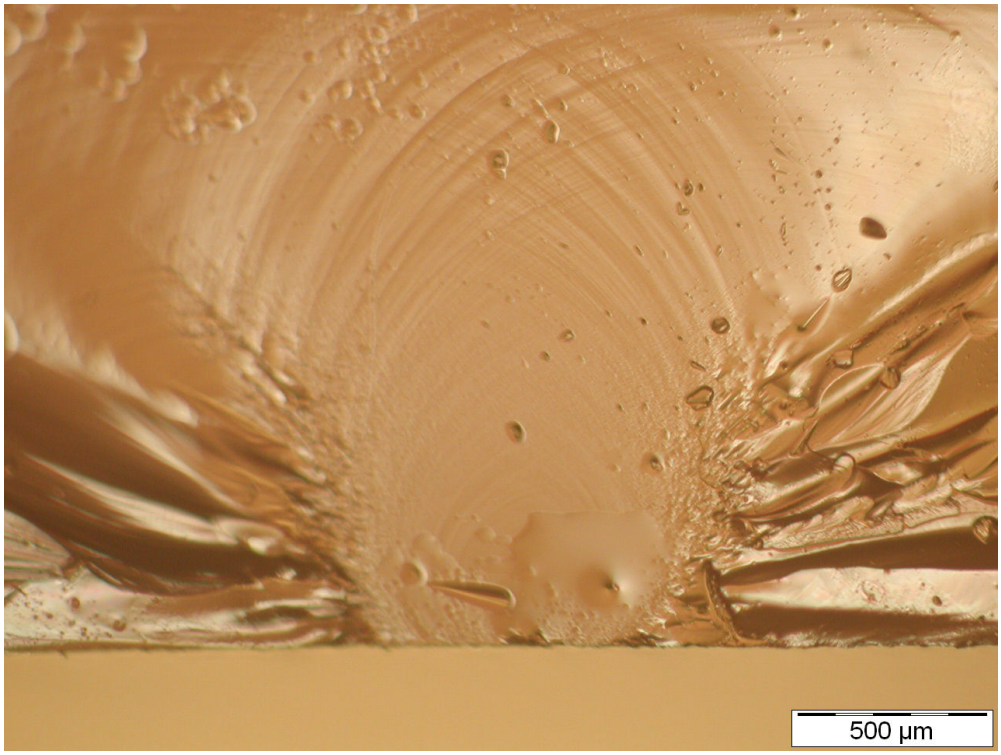

Fig. 3 Fracture surface of an annealed specimen rested in silicon oil, series (1) in Fig. 2.

Under the assumption of half-penny shaped initial cracks, the average depth a_0 of the introduced crack during grinding, can be calculated from K_{Ic} and the measured strength, σ_c.

$$a_0 = \left(\frac{K_{Ic}}{\sigma_c Y} \right)^2 \tag{25}$$

By using $Y \cong 1.3$ and K_{Ic}=0.8 MPa√m we obtain $\boldsymbol{a_0}$**=35 µm**.

3.2.2 Water-soaked specimens

Two series of specimens were then hot water soaked for 24h at 250°C in an autoclave. Drying the specimens in vacuum removed remove surface moisture. After 2 days of drying at 60°C in vacuum, the average strength in silicon oil (series 2) was found to be σ_c=119.7 MPa (SD 9.9 MPa). After drying for 5h at 200°C (series 3) the strength in silicon oil was σ_c=118.0 MPa (SD 12.9 MPa) exhibiting no significant change by the drying procedure. This indicates that 200 °C is not enough to drive the water off [5].

The load-displacement curves obtained in the strength tests in silicon oil were completely different from those obtained from the specimens that were not exposed to saturated steam at 250 °C. Only the unexposed annealed specimens showed the usual straight displacement versus load behaviour until failure. All specimens exposed to water at 250 °C showed popins as schematically indicated in Fig. 4, accompanied by clearly audible cracking noise.

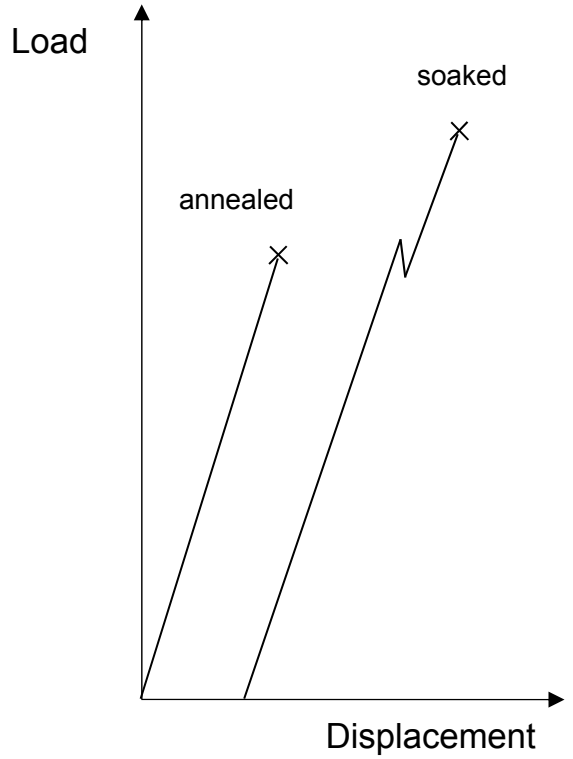

Fig. 4: Load displacement plots in silicon oil. The water-soaked specimens showed a load pop-in that was missing in the tests on unsoaked bars.

The fracture surface of one such test specimen is shown in Fig. 5a and Fig. 5b. Figure 5b represents the fracture origin. At this magnification, the initial crack of depth $a \cong 31\,\mu m$ is

clearly visible. The same holds for the increased crack after the load pop in. The arrest contour gives a new depth of 48µm from which later final fracture starts. Since the crack ends at the surface are not visible, the evaluation is limited here to the deepest points of the cracks, represented by semi-circular surface cracks with $a/c = 1$.

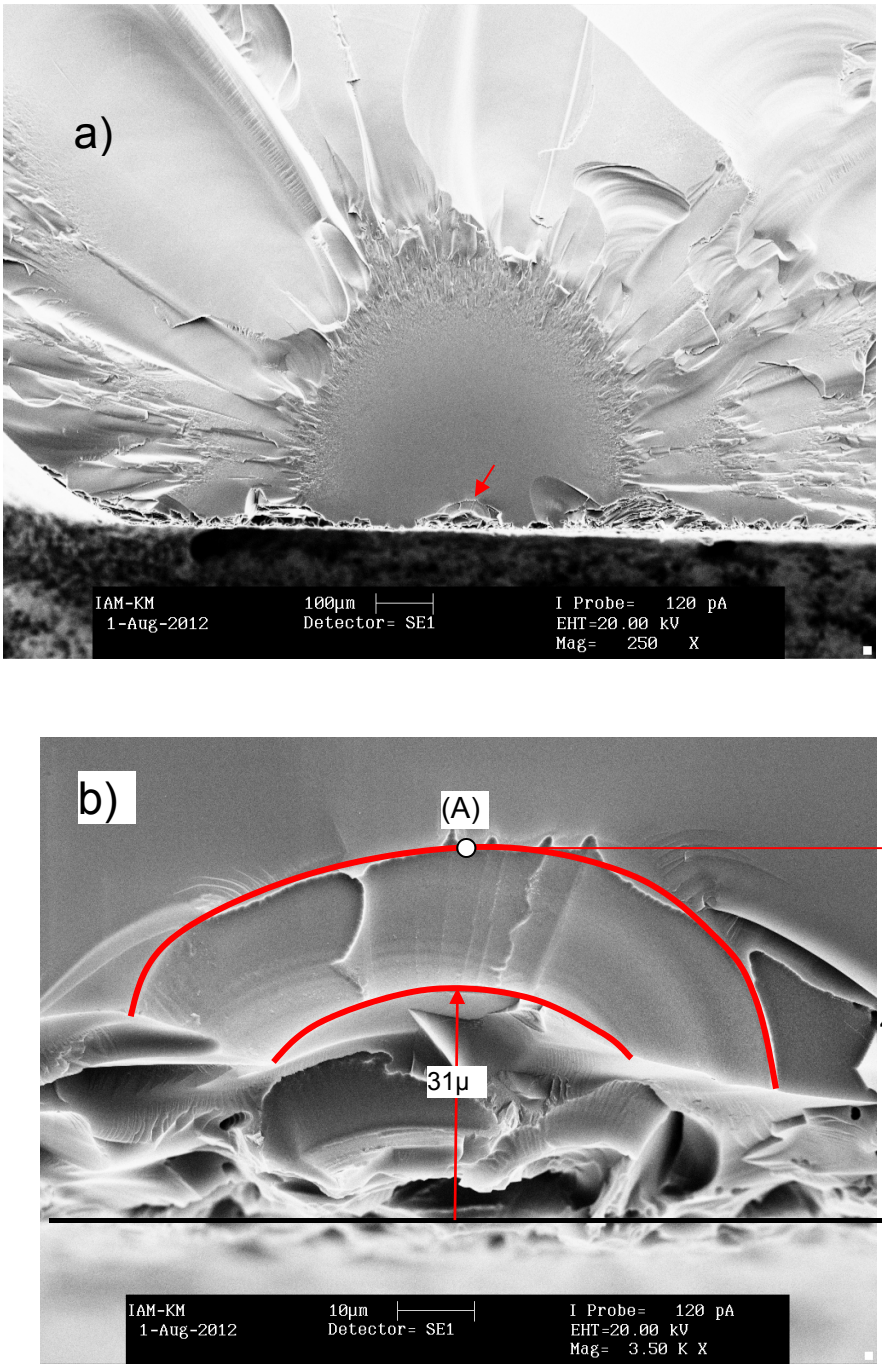

Fig. 5 Fracture surface of a water-soaked specimen measured in silicon oil, a) overall view, b) identification of the initial crack size $a_0 \cong 31$ µm and the extended crack after the pop-in (a=48µm).

The stress intensity factors related to the failure stress can be computed by results of Newman and Raju [13]. Their solution was originally derived for the case of straight specimen surfaces, nevertheless, this solution can also be used for cylindrical specimens if the crack depth is small compared with the cylinder radius R, $a/R << 1$. Since the initial natural surface cracks are very small compared to the specimen thickness W, $a/W << 1$, the solution holds for the stress intensity factor at the deepest point (A) of the semi-circle,

$$K_{appl,A} = \sigma_{appl} 1.173 \sqrt{a} \,. \tag{26}$$

From the strength of $\sigma_f = 119.7$ MPa and the outer crack contour a_c=48 µm at which catastrophically failure starts, we obtain $K_{appl,A} = 0.97$ MPa√m, that is slightly above the fracture toughness of $K_{Ic} = 0.8$ MPa√m [14]. This results in a shielding term at the deepest point of the critical crack of $K_{sh} = 0.97–0.8 = –0.17$ MPa√m.

The applied stress intensity factor at which the crack extended from its original depth of $a_0 \cong 31$µm occurred at about 80-85% of the strength, i.e. at the stress where the load pop-in was observed. This results in an applied stress intensity factor of $K_{appl,A} \approx 0.61$-0.63 MPa√m that is clearly below K_{Ic}. Consequently, crack extension from a_0 to a_c must be caused by subcritical crack growth. The fracture behaviour, Fig. 5b, will be addressed below in the discussion section.

3.3 Bending strength in water

Bending strength measurements in water were carried out for the annealed samples and the 24h/250°C hot-water soaked samples. The mean strength of the annealed samples was σ_f = 70.2 MPa (SD 6.2 MPa), series (4) in Fig. 6. The soaked samples showed a mean failure stress of σ_f = 101.2 MPa (SD 9.2 MPa), series (5) in Fig. 6. In both cases, the load vs. displacement curves continuously increased with increasing load.

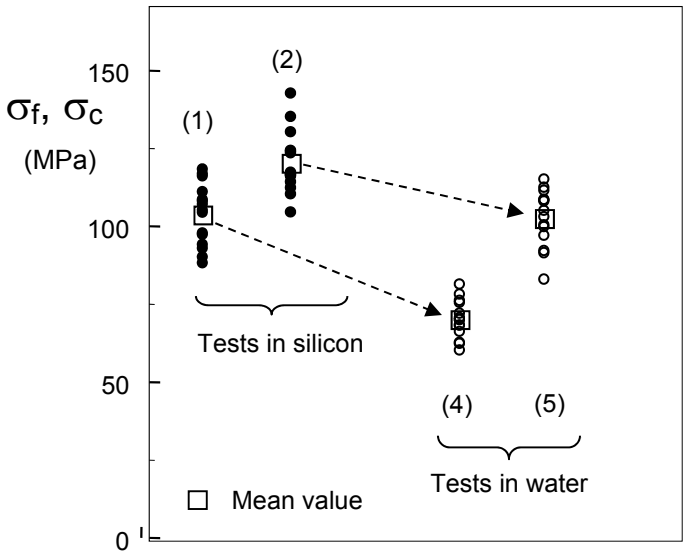

Fig. 6 Bending strengths of annealed and water-soaked silica specimens tested in water.

3.4 Annealing after water soaking

In an additional test, 250°C/24h water-soaked specimens were annealed at 1160°C/2h in vacuum and fractured in silicon oil (series (6) in Fig. 7). By additional annealing, all swelling stresses should be removed and most of the water should be driven out of the glass surfaces. From this point of view, the final strengths should agree with the inert strength of the untreated silica. The measured strength of 94.8MPa (SD 12.1 MPa) are below the strengths for the untreated specimens, 103.5 MPa (SD 9.2 MPa), however, the standard deviations strongly overlap. All measured strengths are once more compiled in Table 1.

Series	Mean strength	Standard deviation	Procedure
(1)	103.5	9.2	Untreated//silicon oil
(2)	119.7	9.9	Water soaked//65°C dried
(3)	118.0	12.9	Water soaked//200°C dried
(4)	70.2	6.2	Untreated//test in water
(5)	101.2	9.2	Water soaked//test in water
(6)	94.8	12.1	Water soaked//annealed// silicon oil

Table 1 Mean values and standard deviations of 4-point bending strengths on rectangular bars.

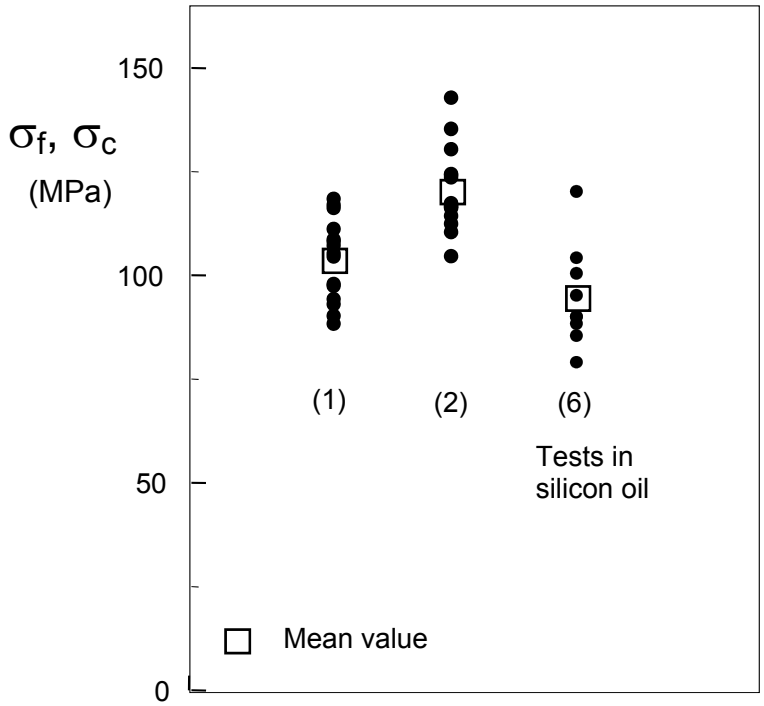

Fig. 7 Water-soaked specimens (250°C, 24h) stress-free annealed after soaking for 2h at 1160°C, then fractured in silicon oil, series (6).

The differences of the mean strength values for the experiments in silicone oil (Fig. 2) were tested by means of a *Student T-Test* analysis. The unsoaked series (1) compared with the soaked series (2) yields a probability that there would be no statistically significant difference between the two series of p=0.021%. This is a very low probability, so that the assumption that the strengths are significantly different is a good assumption.

The same result holds for the tests on unsoaked and soaked silica tested in water, series (4) and (5), respectively. In this case, the probability for equal mean values is only $1.3\ 10^{-6}$ %. The increased strength by soaking is significant.

Finally, it can be shown by comparing series (1) with series (6), both measured in silicone oil, that after 1150°C annealing in vacuum the whole strength excess due to soaking disappeared.

Series	Series	Probability for equality	Conclusion
(1)	(2)	p=0.021 %	Soaked and unsoaked series in silicone oil are significantly different
(4)	(5)	$p=1.3\ 10^{-6}$ %	Soaked and unsoaked series in water oil are significantly different
(1)	(6)	p=6.7 %	After 1h vacuum annealing at 1150°C initially and unsoaked specimens are not significantly different

Table 2 Comparisons between several test series by two-tail Student-t-test.

4. Discussion of pop-in behaviour

4.1 Water occurrence for subcritical crack growth in silicon oil tests

Measurements in silicon oil resulted in real inert strengths only in the case of the annealed un-soaked specimens. In strength tests on soaked specimens, also carried out in silicon oil, we found clear evidence for subcritical crack growth, even though the environment had prevented any water supply.

Now let us look for a water source in the absence of any supply from the environment. Water that diffused into silica during the water soaking procedure reacts with the silica network according to Eq. 3.

For 250 °C, the ratio S/C is about 2.8, Eq. 6. The percentage of molecular water is then $C/(S/2+C) \approx 42\%$. From the measurements by Zouine et al. [7] we get from Eq. 3 by a slight temperature extrapolation to 250°C a *total water* concentration at the surface of

$C_w \approx 5.5\times10^{20}$ molecules of H_2O/cm^3. Consequently, the surface concentration of molecular water is $C \approx 0.42\times5.5\times10^{20} \approx 2.3\times10^{20}$ molecules of *molecular* H_2O/cm^3.

This shows that molecular water, necessary for bond splitting during subcritical crack growth is in the soaked specimens always available ahead of a crack tip. The distribution of molecular water after 24h soaking at 250°C is illustrated in Fig. 8. Under these soaking conditions it results from Eqs. 1 and 2: $b = 6.3$ µm shown in Fig. 8 by the dashed contour.

The C-profile along the x-axis as the prospective crack plane is concluded from FE-results in [3]. The content of molecular water is negligible for $x > 3b$.

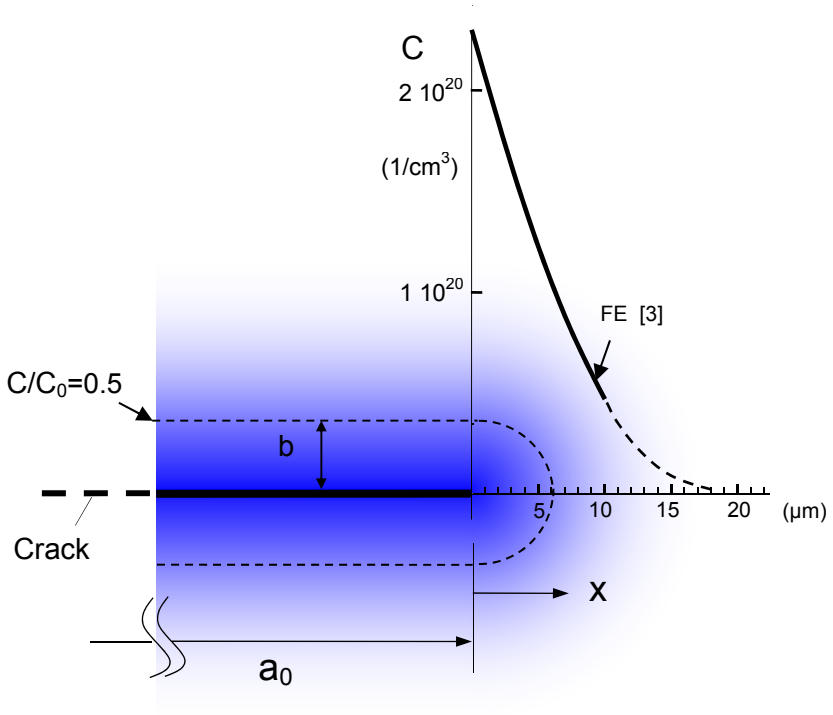

Fig. 8 Distribution of molecular water in the surrounding of a crack tip after 24h water soaking at 250°C.

For strength tests in water, crack growth is also strongly accelerated by the effect of water escaping from the initial swelling zone. However, in contrast to the silicon oil tests, there is now no crack arrest possible since water is always available to the advancing crack tip from the surrounding environment. Consequently, in these tests accelerated cracking is directly followed by final fracture without any further increase of loading necessary. The pop-in is therefore missing.

4.2 Interpretation of crack extension accompanied by load pop-ins

A side-view of the semi-circular surface crack is shown in Fig. 9a. From all surfaces that are in contact with water vapour during high-temperature soaking, water diffuses into the silica. This holds also for the crack surfaces. For reasons of transparency in the computation of the shielding stress intensity factor, these contours are approximated by a zone of constant thickness b ending in a half-circle.

If the crack grows under increasing load by an amount of Δa, it will escape from the initial swelling zone, as illustrated by the dashed crack extension. The related shielding stress intensity factor is schematically plotted in Fig. 9b as a function of crack propagation Δa. When $\Delta a = b$ is reached and the crack tip leaves the swelling zone, the shielding stress intensity factor strongly decreases as was shown for ion-exchange layers in [15].

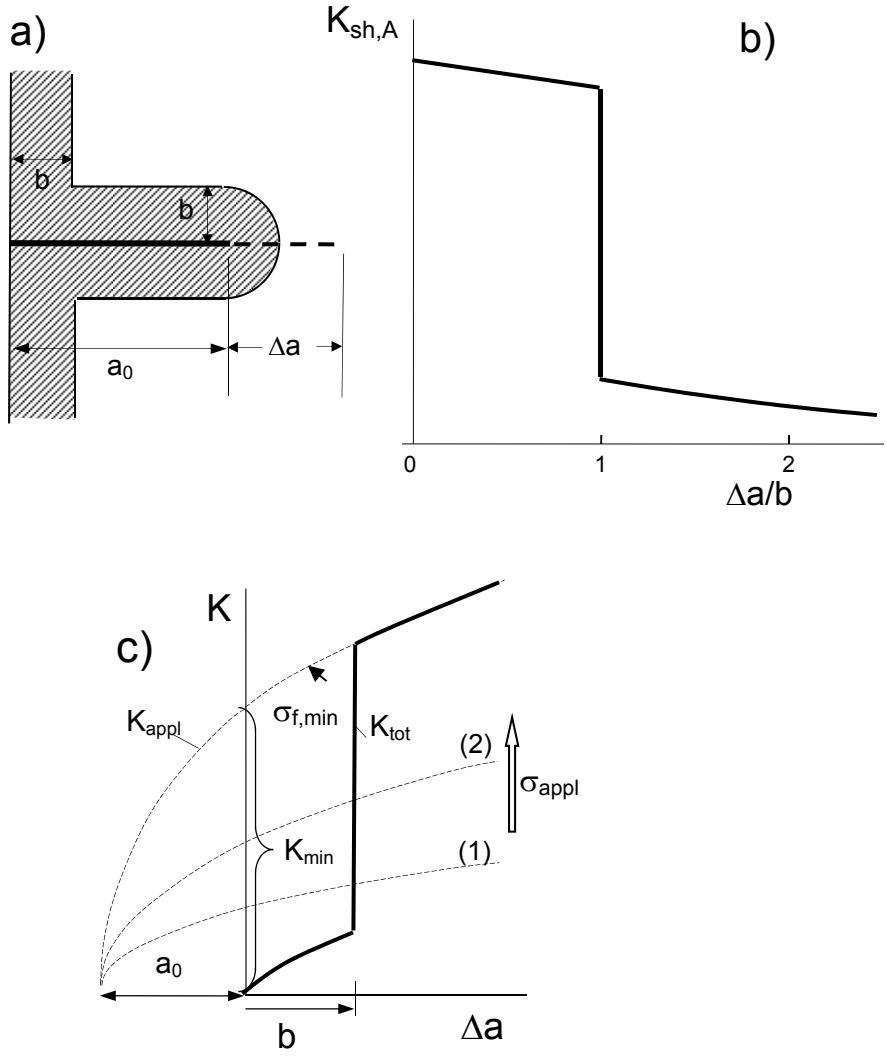

Fig. 9 a) Crack propagating out of the initial swelling zone, b) shielding stress intensity factor during crack escape, c) increase of the total stress intensity factor K_{tot} during crack growth for three applied loads (schematic). Below the applied stress $\sigma_{appl}=\sigma_{f,min}$ defining a lower limit for measurable strengths, no subcritical crack growth is possible because of $K_{tot}<0$.

Superposition of the applied stress intensity factor $K_{appl} \propto \sqrt{a}$ (dashed curve in Fig. 9c) and the shielding stress intensity factor K_{sh} results in the total stress intensity factor K_{tip} as given by Eq. 11.

The development of K_{tip} with increasing crack length, $a_0+\Delta a$, and increasing load is schematically shown in Fig. 9c by the solid curve. Under increasing load the first positive

total stress intensity factor, $K_{min} = -K_{sh}$, is reached at $\Delta a = 0$ for the curve indicated by $\sigma_{f,min}$ which is the minimum possible strength in a dynamic strength tests

$$\sigma_{f,\min} = \frac{-K_{sh}}{1.17\sqrt{a_0}} \tag{27}$$

From the shape of the K_{tip} - Δa - curve, it is evident that a crack extension by subcritical crack growth must accelerates rapidly in the region where K_{tip} increases rapidly, namely at $\Delta a \geq b$. On the other hand, we have to take into consideration the fact that simultaneously with the loss of shielding also the available water for subcritical crack growth disappears after a crack extension of about $\Delta a \approx b$. This results in an abruptly arresting crack so far $K_{tip} < K_{Ic}$. Final cracking can occur only after a sufficient increase of the loading. This trivially must result in the observed load-displacement curve of Fig. 4.

4.3 Interpretation of the shieldig stress intensity factor

The shielding stress intensity factor at the deepest point of a semi-circular surface crack soaked from the side surface and the crack surfaces, Fig. 9a, is given by [16]

$$K_{sh,A} \cong -1.17\sqrt{a}\,\frac{\varepsilon_v E}{3(1-\nu)}\tanh\left(0.698\sqrt{\frac{b}{a}} + 0.317\frac{b}{a}\right) \tag{28}$$

For the crack with depth of $a = 48$ µm and a volume strain at 250°C of $\varepsilon_v = 0.81\%$ given. By Eq. 7, it results from (28) with $b = 6.3$ µm, $E = 72$ GPa and $\nu = 0.17$:

$$K_{sh} = -0.54\ \text{MPa}\sqrt{\text{m}} \tag{29}$$

This is in contrast to the result evaluated in Section 3.2. From the experiment we found a shielding term at the deepest point of the critical crack of only $K_{sh} \cong -0.17$ MPa√m, i.e. 31% of the expected result, Eq. 29. The reason for this difference is that Eq. 28 holds for a crack that is fully surrounded by the swelling zone as is schematically shown in Fig. 9a. If the crack is not fully surrounded, two contributions make up the shielding stress intensity factor: one coming from the diffusion zone originating from the crack faces, $K_{sh,1}$, the second originating from the external surfaces of the specimen, $K_{sh,2}$. For a transparent interpretation of this situation let us apply the K-separation according to [16]. The total shielding stress intensity factor is the sum

$$K_{sh} = K_{sh,1} + K_{sh,2} \tag{30}$$

The stress intensity factor by the side surface is shown in Fig. 10 as a function of b/a and the crack aspect ratio a/c ($2c$ = width of the crack). In our case results for $a/c = 1$ and $b/a = 6.3\mu\text{m}/48\mu\text{m} = 0.13$ (circle in Fig. 10), we find that $K_{sh,2} = -0.095$ MPa√m.

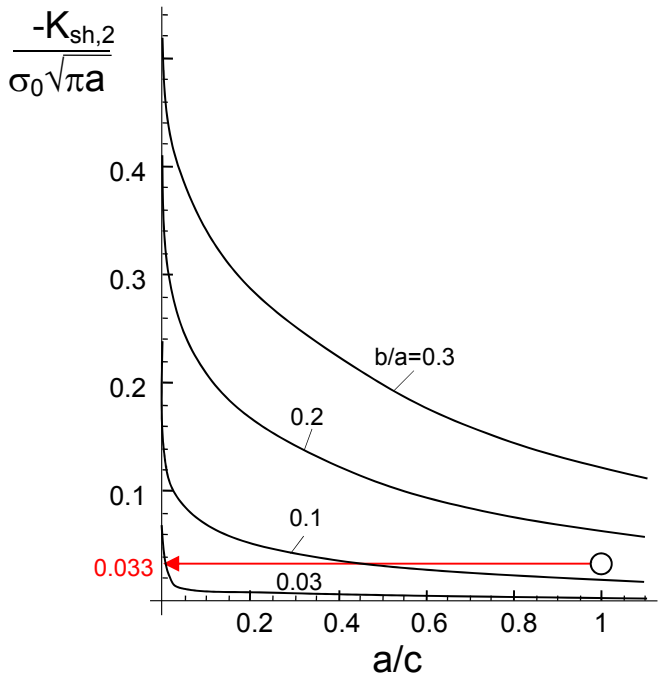

Fig. 10 Influence of aspect ratio a/c and relative depth of the swelling zone b/a on the shielding stress intensity factors K_{sh} at the deepest point of a semi-elliptical surface crack [16].

When the crack can grow subcritically by an amount of Δa, it will escape from the initial swelling zone, as illustrated in Fig. 11. The stress intensity factor $K_{sh,1}$ for the swelling zone developing from the crack faces, is shown in Fig. 11 as given in [17], Fig. I 5.6.

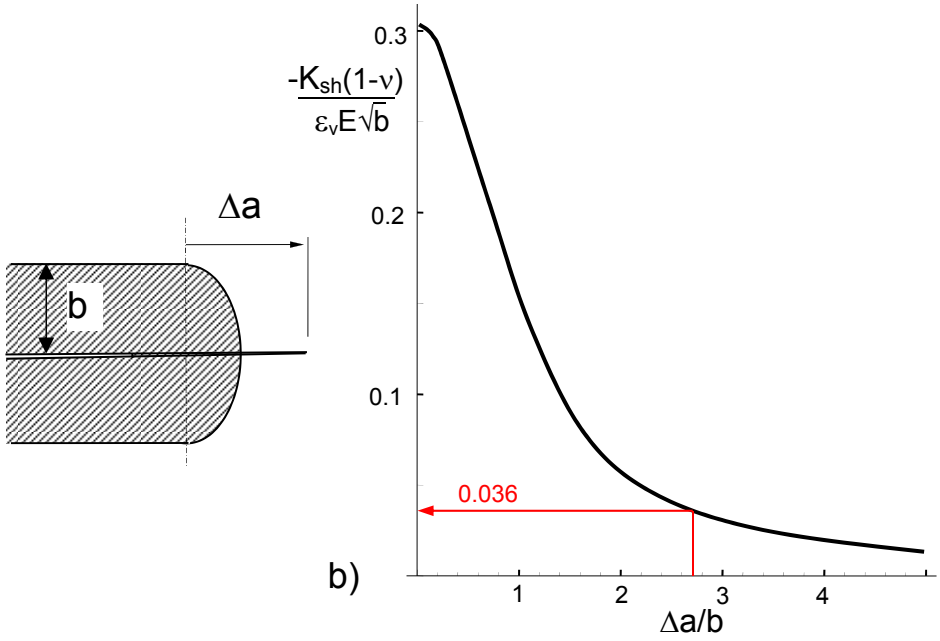

Fig. 11 Shielding stress intensity factor $K_{sh,1}$ for a crack growing out of the initial swelling zone, from [17].

The shielding stress intensity factor $K_{sh,1}$ for an extension of Δa =48 -31 µm = 17 µm and $\Delta a/b$ = 2.7 decreases (red arrow in Fig. 11) to a normalized stress intensity factor of 0.036. Consequently, the following equation is obtained for $K_{sh,1}$:

$$K_{sh,1} = -0.036 \frac{\varepsilon_v E}{1-\nu} \sqrt{b} = -0.0634\,\text{MPa}\sqrt{\text{m}} \qquad (31)$$

The total shielding term after 17µm crack extension calculated from Eq. 30 as

$$K_{\text{sh}} = -0.0634\ \text{MPa}\sqrt{\text{m}} - 0.095\ \text{MPa}\sqrt{\text{m}} = -0.157\,\text{MPa}\sqrt{\text{m}}$$

is in fairly good agreement with the experimental value of $-0.17\,\text{MPa}\sqrt{\text{m}}$.

Summary:

The present study deals with the influence of swelling and shielding in silica caused by the reaction between SiO_2 and water.

- In the first part we considered the effect of swelling stresses on the crack-growth exponent, n', of the power-law for subcritical crack growth. It could be shown that the apparent exponent n' of a power law description crack growth,

  $$v \propto K_{appl}^{n},$$

  must decrease with increasing swelling. This theoretical consequence of swelling in silica is in good agreement with experiments from literature.

- In the second part, strength tests on soaked versus un-soaked specimens are reported, which were carried out in silicone oil or in humid environments (lab air and water)

  Soaked specimens showed an increased strength for the tests in both oil and water, as could be proved by means of a *Student t-Test* analysis.

  After annealing at 1150°C in vacuum the strength excess due to soaking disappeared, most likely a consequence of water being driven out of the glass, thus eliminating the shielding stresses.

  For the soaked specimens load "pop-ins" appeared that could be interpreted by evaluation of crack contours. The reason for this behavior is discussed in terms of fast subcritical crack growth in the water-containing soaking zone ahead of the crack tip.

References:

1. S.M. Wiederhorn, T. Fett, G. Rizzi, S. Fünfschilling, M.J. Hoffmann and J.-P. Guin, "Effect of Water Penetration on the Strength and Toughness of Silica Glass," *J. Am. Ceram. Soc.* **94** (2011) [S1], 196-203.

2. S.M. Wiederhorn, T. Fett, G. Rizzi, M.J. Hoffmann and J.-P. Guin, "The Effect of Water Penetration on Crack Growth in Silica Glass," *Engng. Fract. Mech.* **100** (2013), 3-16.

3. S.M. Wiederhorn, T. Fett, G. Rizzi, M. Hoffmann, J.-P. Guin, "Water Penetration – its Effect on the Strength and Toughness of Silica Glass," *Met. Mater. Trans. A*, **44**(2013) [3], 1164 -1174.

4. T. Fett, G. Rizzi, M. Hoffmann, and S.M. Wiederhorn, "Effect of Water on the inert Strength of Silica Glass: Role of Water Penetration," *J. Am. Ceram. Soc.* **94**(2011) [6], S196-S203.

5. H. Li and M. Tomozawa, "Mechanical strength increase of abraded silica glass by high pressure water vapor treatment," *J. Non-Cryst. Solids* **168**(1994), 287-292.

6. S. Wagner, B. Hohn, D. Creek, M.J. Hoffmann, G. Rizzi, S.M. Wiederhorn, T. Fett, Strength measurement on silica soaked in hot water, KIT Scientific Working Papers, ISSN: 2194-1629**,** 2014.

7. Zouine, A., Dersch, O., Walter, G., Rauch, F., Diffusivity and solubility of water in silica glass in the temperature range 23-200°C, *Phys. Chem. Glasses,* **48** (2007), 85-91.

8. R.H. Doremus, "Diffusion of water in silica glass," *J. Mater. Res.*, **10** 2379-2389 (1995).

9. Oehler, A., Tomozawa, M., Water diffusion into silica glass at a low temperature under high water vapor pressare, J. Non-Cryst. Sol. **347**(2004) 211-219.

10. S. M. Wiederhorn, F. Yi, D. LaVan, T. Fett, M.J. Hoffmann, Volume Expansion caused by Water Penetration into Silica Glass, *J. Am. Ceram. Soc.*, in press.

11. D. Munz and T. Fett, *Ceramics, Mechanical Properties, Failure Behavoour, Matrials Selection*, Springer-Verlag (1999)

12 V.M. Sglavo and D.J. Green, "Fatigue limit in fused silica," J. Eur. Cram. Soc. **21** (2001) 561-567.

13. J.C. Newman and I.S. Raju, "An empirical stress intensity factor equation for the surface crack," *Engng. Fract. Mech.* **15,** 185-192, (1981).

14 S.M. Wiederhorn, Fracture surface energy of glass, J. Am. Ceram. Soc. **52** (1969), 99-105.

15 Fett, T., Guin, J.P., Wiederhorn, S.M., Interpretation of effects at the static fatigue limit of soda-lime-silicate glass, Engng. Fract. Mech. **72**(2005), 2774-279**.**

16 T. Fett, G. Rizzi, M. Hoffmann, S. Wagner, and S.M. Wiederhorn, "Effect of Water on the inert Strength of Silica Glass: Role of Water Penetration," *J. Am. Ceram. Soc.* **95**(2012) [12], 3847-3853.

17 T. Fett, New contributions to R-curves and bridging stresses – Applications of weight functions, IAM 3, KIT Scientific Publishing, 2012, Karlsruhe.

KIT Scientific Working Papers
ISSN 2194-1629

www.kit.edu